7-2020

Optimization of Railroad Bearing Health Monitoring System for Wireless Utilization

Jonas Cuanang
The University of Texas Rio Grande Valley

Constantine Tarawneh
The University of Texas Rio Grande Valley

Martin Amaro Jr.
The University of Texas Rio Grande Valley

Jennifer Lima
The University of Texas Rio Grande Valley

Heinrich D. Foltz
The University of Texas Rio Grande Valley, heinrich.foltz@utrgv.edu

Recommended Citation

Cuanang, J, Tarawneh, C, Amaro, M, Jr., Lima, J, & Foltz, H. "Optimization of Railroad Bearing Health Monitoring System for Wireless Utilization." Proceedings of the 2020 Joint Rail Conference. 2020 Joint Rail Conference. St. Louis, Missouri, USA. April 20–22, 2020. V001T03A007. ASME. https://doi.org/10.1115/JRC2020-8060

Proceedings of the 2020 Joint Rail Conference
JRC2020
April 20-22, 2020, St. Louis, MO, USA

JRC2020-8060

OPTIMIZATION OF RAILROAD BEARING HEALTH MONITORING SYSTEM FOR WIRELESS UTILIZATION

Jonas Cuanang
Department of Mechanical Engineering
University of Texas Rio Grande Valley
Edinburg, TX, 78539, USA
jonas.cuanang01@utrgv.edu

Constantine Tarawneh, Ph.D.
Department of Mechanical Engineering
University of Texas Rio Grande Valley
Edinburg, TX, 78539, USA
constantine.tarawneh@utrgv.edu

Martin Amaro Jr.
Department of Mechanical Engineering
University of Texas Rio Grande Valley
Edinburg, TX, 78539, USA
martin.amaro01@utrgv.edu

Jennifer Lima
Department of Mechanical Engineering
University of Texas Rio Grande Valley
Edinburg, TX, 78539, USA
jennifer.lima01@utrgv.edu

Heinrich Foltz, Ph.D.
Department of Electrical and Computer Engineering
University of Texas Rio Grande Valley
Edinburg, TX, 78539, USA
heinrich.foltz@utrgv.edu

ABSTRACT

In the railroad industry, systematic health inspections of freight railcar bearings are required. Bearings are subjected to high loads and run at high speeds, so over time the bearings may develop a defect that can potentially cause a derailment if left in service operation. Current bearing condition monitoring systems include Hot-Box Detectors (HBDs) and Trackside Acoustic Detection Systems (TADS™). The commonly used HBDs use non-contact infrared sensors to detect abnormal temperatures of bearings as they pass over the detector. Bearing temperatures that are about 94°C above ambient conditions will trigger an alarm indicating that the bearing must be removed from field service and inspected for defects. However, HBDs can be inconsistent, where 138 severely defective bearings from 2010 to 2019 were not detected. And from 2001 to 2007, Amsted Rail concluded that about 40% of presumably defective bearings detected by HBDs did not have any significant defects upon teardown and inspection. TADS™ use microphones to detect high-risk bearings by listening to their acoustic sound vibrations. Still, TADS™ are not very reliable since there are less than 30 active systems in the U.S. and Canada, and derailments may occur before bearings encounter any of these systems.

Researchers from the University Transportation Center for Railway Safety (UTCRS) have developed an advanced algorithm that can accurately and reliably monitor the condition of the bearings via temperature and vibration measurements. This algorithm uses the vibration measurements collected from accelerometers on the bearing adapters to determine if there is a defect, where the defect is within the bearing, and the approximate size of the defect. Laboratory testing is performed on the single bearing and four bearing test rigs housed at the University of Texas Rio Grande Valley (UTRGV). The algorithm uses a four second sample window of the recorded vibration data and can reliably identify the defective component inside the bearing with up to a 100% confidence level. However, about 20,000 data points are used for this analysis, which requires substantial computational power. This can limit the battery life of the wireless onboard condition monitoring system. So, reducing the vibration sample window to conduct an accurate analysis should result in a more optimal power-efficient algorithm. A wireless onboard condition monitoring module that collects one second of vibration data (5,200 samples) was manufactured and tested to compare its efficacy against a wired setup that uses a four second sample window. This study investigates the root-mean-square values of the bearing vibration and its power spectral density plots to create an optimized and accurate algorithm for wireless utilization.

INTRODUCTION

A freight railcar's cargo load is supported by its suspension system that consists of springs, dampers, axles, wheels and tapered-roller bearings. Due to the heavy cargo that railcars carry at relatively high speeds, the bearings are the most susceptible to catastrophic failure leading to journal burn-off.

Tapered-roller bearings on freight railcars allow near-frictionless operating conditions based on normal operation of

the three fundamental components: inner rings (cones), outer ring (cup), and rollers, shown in Figure 1. However, once one of these components develops a defect, the near-frictionless design is compromised, which can lead to increased frictional heating depending on the defect size and location.

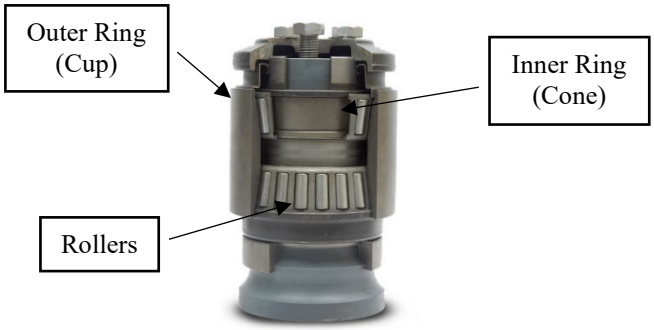

Figure 1. Tapered-Roller Bearing Components [1].

Bearing defect types can be categorized as a localized defect, distributed defect, or geometric defect. Pictured in Figure 2, localized defects include pits, cracks, or spalls, while distributed defects can be found on multiple components with localized defects or a single component with multiple defects that are distributed throughout its surface, such as a water-etch defect. Geometrical defects usually result from faults in the manufacturing processes that cause one or multiple bearing components to be out of tolerance.

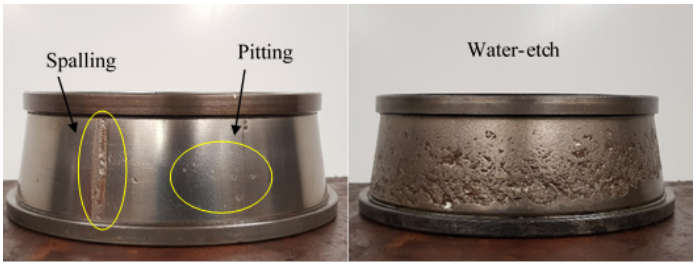

Figure 2. Example of a localized defect (left) and distributed defect (right).

Bearing Condition Monitoring Systems

Current railway bearing condition monitoring systems include Hot-Box Detectors (HBDs) and Trackside Acoustic Detection Systems (TADS™). These systems are considered wayside devices that are mounted adjacent to the rail tracks to monitor the health of freight railcar bearings as they pass by these devices.

With over 6,000 in use in the United States and Canada, the HBDs are the most utilized bearing condition monitoring systems operating in North America. Depending on the amount of traffic on the rail lines, HBDs can be placed anywhere between 40 km (25 miles) to 64 km (40 miles) apart. HBDs measure the radiated temperatures from railcar bearings, wheels, axles, and brakes with non-contact infrared sensors. The railcar conductor would be alerted if the temperature of any bearing is detected to be greater than 94.4°C (170°F) above ambient conditions or if a bearing is running 58.3°C (105°F) hotter than its axle mate. A more conservative approach utilized by many railroads classifies bearings that are operating above the average temperature of all bearings on the same side of the train as "warm trending" bearings [2]. Warm-trending bearings are flagged without triggering any of the HBD alarms and are later removed from service for disassembly and inspection.

TADS™ utilizes wayside microphones to detect high-risk defects in bearings and can alert the conductor as the train passes by the system. One example of a high-risk defect is a "growler". Growlers are defective bearings in which spalls occupy about 90% of the bearing component's rolling surface area. Although TADS™ is very proficient in determining end-of-life bearings, there are only 30 systems that are in service in both the United States and Canada, and these are heavily concentrated in the East. In addition, even though TADS™ can identify high-risk defects in bearings, they cannot detect other defects that are much smaller in size [3]. Thus, not only will most bearings in service never pass through a TADS™ system in their lifespan, but those that do will go undetected if the defect size is small compared to a growler.

The UTCRS research team completed a study in which the temperature profiles of healthy or defect-free bearings were compared to bearings with defects in either the inner (cone) or outer (cup) ring [4]. The study demonstrated that bearings with defective inner or outer rings operated at similar temperatures when compared to healthy bearings with no defects, thus, indicating that the operating temperature is not a good predictor of bearing health [4]. Thus, the research team focused on developing an advanced onboard condition monitoring device that captures the vibration signatures within the bearing using an accelerometer. This device utilizes the detected vibration levels to assess the health of the bearing and the stage of deterioration of the bearing's raceways [5]. This study will combine new research findings that correlate defect size with bearing vibration levels and recently published data [6] to provide proof of concept validation for the wireless onboard condition monitoring device.

EXPERIMENTAL SETUP & PROCEDURES

The University Transportation Center for Railway Safety (UTCRS) owns a Single Bearing Test Rig (SBT), pictured in Figure 3, that was specifically designed and fabricated to simulate the operation conditions for a Class K (6½"×9"), Class F (6½"×12"), Class G (7"×12"), or Class E (6×11") tapered-roller bearing in field service. This test rig has the test bearing cantilevered at the end of the axle to closely mimic the loading conditions in a freight railcar. In a fully loaded railcar, each bearing experiences a load of 153 kN (34.4 kip) for Class F and K bearings. The SBT utilizes a hydraulic cylinder that can apply loads up to 150% of a fully loaded railcar. The experimental data presented in this paper were acquired from two loading conditions, namely, 17% of full load representing an empty railcar, and 100% of full load representing a fully loaded railcar. The SBT uses a 22 kW (30 hp) variable frequency motor that allows the bearing to replicate railway wheelset speeds up to 137

km/h (85 mph). Two industrial size fans are used to cool the bearings with an average air stream of 6 m/s (13.4 mph). Bearings containing a spall on the outer ring (cup) raceway are positioned so that the spall is located under the direct path of the applied load (i.e., the 90º position shown in Figure 4). This is done to induce a worst-case scenario operating condition where the defective area is subjected to the maximum load in order to cause the defect to propagate as fast as possible.

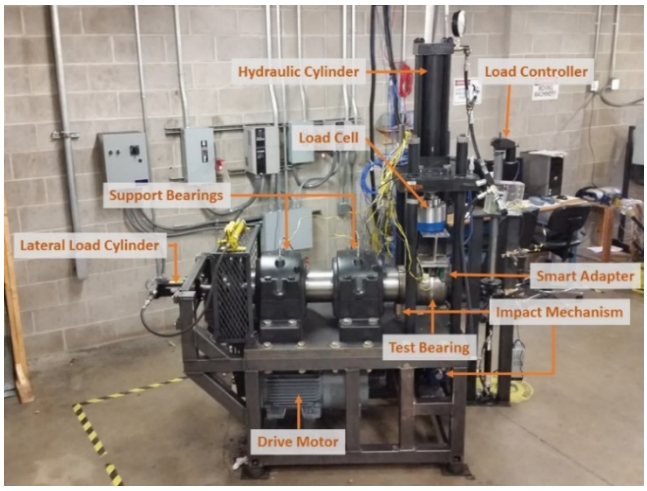

Figure 3. Single Bearing Test Rig (SBT) [7]

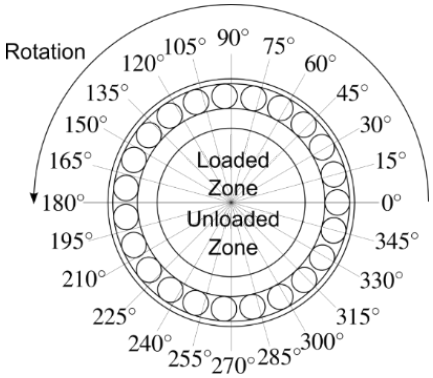

Figure 4. Bearing schematic and spall placement locations.

A bearing adapter was specifically machined to accommodate mounting of three 70g accelerometers, one 500g accelerometer, as well as the developed wireless onboard condition monitoring module. As shown in Figure 5, on the inboard side of the bearing, two wired 70g accelerometers were mounted at the Smart Adapter (SA) and Mote (M) locations. On the outboard side of the bearing, one wired 70g accelerometer as well as the wireless module that utilizes a 100g accelerometer were mounted at the Smart Adapter (SA) location, whereas, the 500g accelerometer was mounted at the Radial (R) location. The battery pack that powers the wireless module was mounted on the Mote (M) location on the outboard side of the bearing, as pictured in Figure 5. Additionally, four K-type bayonet thermocouples were affixed to the bearing adapter on the inboard and outboard sides to monitor the temperature of the bearing at each raceway.

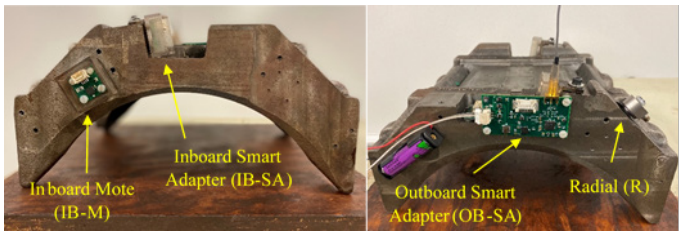

Figure 5. Modified bearing adapter showing sensor locations.

In this study, all the data was collected and recorded using a National Instruments (NI) PXIe-1062Q data acquisition system (DAQ) which was programmed using LabVIEW™. The thermocouple temperature data was collected using a NI TB-2627 card in which a sampling rate of 128 Hz was used to acquire half a second of data every twenty-second interval. For the accelerometer data on the wired setup, an 8-channel Ni PXI-4472B card was used in which a sampling rate of 5,120 Hz was utilized to collect sixteen seconds worth of data in ten-minute intervals. On the wireless setup, a Raspberry Pi 3 Model B+ was used to capture one second worth of accelerometer data via Bluetooth at a sampling rate of 5,200 Hz once every ten-minute interval. The data collected during a planned experiment is later analyzed using the mathematical software Matlab™ to acquire the root-mean-square (RMS) values of the accelerometer data as well as the frequency spectrums.

The vibration levels within a bearing were closely tracked and monitored by the various installed accelerometers. If the RMS value for the bearing exceeded the typical threshold for a healthy bearing, the experiment was stopped, and the bearing was pressed off the axle and disassembled for a thorough inspection of all its components. If a spall was found one any of the bearing raceways, a casting of the defect was created by surrounding the defective area with sealant (tacky) tape having a melting point of 204°C (400°F). Then, a molten bismuth alloy with a melting temperature of 80°C (176°F) is poured into the cavity created by the tacky tape, as depicted in Figure 6.

Figure 6. Casting procedure using Bismuth alloy; spalled surface outlined with tacky tape (left); Bismuth alloy cast (right).

After hardening, the casting is removed from the mold (cavity) and the spalled region is painted to highlight the defect.

Creating a casting of the defect allows for further analysis and measurements without having to delay experimentation once the bearing has been reassembled and pressed on the axle. The casting is used to measure the defect area. To do so, an image of the painted spall region is obtained, and post-processed utilizing codes created in MATLAB™ which enhance the contrast of the darkened spall region. These images are then imported to Image Pro-Plus® where a digital analysis of the defect is performed through optical techniques to acquire accurate defect area parameters.

RESULTS AND DISCUSSION

A previous study performed by the UTCRS research team concluded that the bearing operating temperature is not a reliable metric to assess bearing health, especially in the early stages of defect initiation and propagation [6]. Results from that study demonstrated that an onboard vibration-based monitoring system would be more accurate for detecting bearing defects even in their early stages of initiation and propagation. Sixteen seconds of vibration data was collected at a sampling rate of 5,120 Hz, but only the first four seconds of data were analyzed by the developed algorithm. Although the computational power required to analyze four seconds of vibration data (20,480 data points) is not an issue of concern in a wired system, it is an important factor to consider in a wireless, battery-operated onboard condition monitoring device. Reducing the amount of data necessary to perform an accurate and reliable assessment of the bearing health will have major implications on the power consumption and battery life of the developed wireless onboard condition monitoring device. This study uses a fabricated prototype wireless onboard condition monitoring module to investigate whether an accurate assessment of a bearing's health can be carried with only a one-second sample window. The condition monitoring algorithm utilizes a three-step process. Step 1 determines if the bearing is healthy or defective (Level 1 analysis); Step 2 determines the type of bearing defect (Level 2 analysis); and Step 3 estimates the approximate size of the bearing defect (Level 3 analysis). However, only Level 1 and Level 2 analyses need to be optimized for wireless utilization.

Experiment 202

In Experiment 202, a class K bearing with a spalled cone (inner ring) raceway at the inboard side of the bearing was run on the single bearing tester (SBT). During the experiment, the cone spall grew to a total area of 10.51 cm^2 (1.63 in^2). A picture of the spall is presented in Figure 7. Ten different speeds at two different loading conditions simulating an empty and a fully loaded railcar were utilized for this experiment.

The temperature and vibration signatures of the test bearing during Experiment 202 are provided in Figure 8. The root-mean-square (RMS) vibration values plotted in Figure 8 were calculated from four seconds of data acquired at a sampling rate of 5,120 Hz every ten-minute interval from four wired 70g accelerometers. It is apparent from the vibration signatures captured by all four accelerometers that the bearing is defective since the RMS values are greater than the maximum RMS threshold for healthy bearings indicated by the solid red line in Figure 8. The inboard smart adapter (IB-SA) accelerometer recorded the highest RMS values, which is not surprising given that the spalled cone resides in the inboard side of the bearing. Interestingly, looking at the temperature profile for this test bearing, it can be seen that the operating temperature of this bearing is consistently lower than the threshold temperature for healthy (control) bearings indicated by the solid red line. The only times the bearing operating temperature exceeded the threshold value is immediately after sudden changes in operating conditions that require some settling time before the bearing operating temperature reaches steady-state conditions. At steady state, the operating temperature of the bearing remains lower than the threshold temperature. This reinforces the conclusion that bearing operating temperature is not a reliable metric for assessing bearing health.

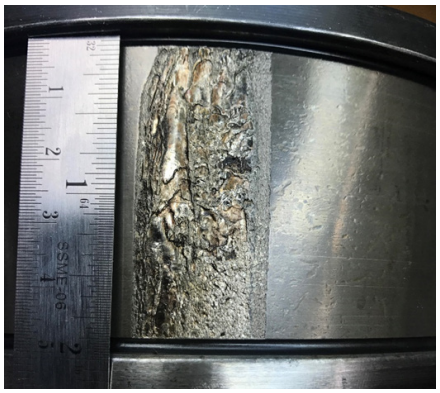

Figure 7. Post-experiment cone spall defect (ruler is in inches).

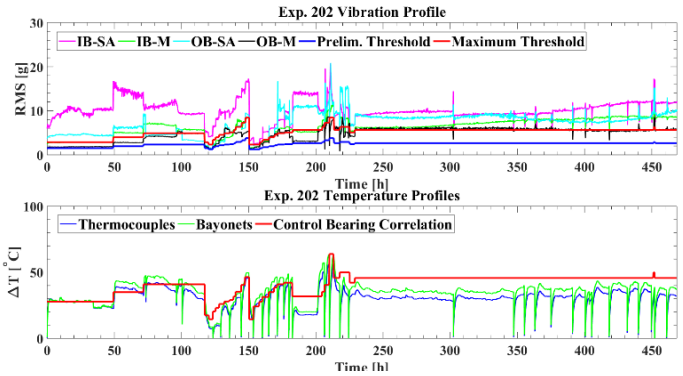

Figure 8. Vibration (4 seconds of data) and temperature profiles for Experiment 202.

Once Level 1 analysis concluded that the bearing is defective, the type of defect was determined by analyzing the power spectral density (PSD) plots of the raw acceleration data. Level 2 analysis uses three fundamentally derived defect frequencies (i.e., f_{cup}, f_{cone}, and f_{roller}) and their harmonics to identify the defect type. The defect frequency with the highest total frequency and harmonics magnitude within a certain frequency range determines the defect type [8]. Specifically, the

percentage of the highest total defect frequency and harmonics magnitude over the sum of magnitudes of all defect frequencies and their harmonics over a definite frequency range must be at least 50% for the algorithm to identify the defect type. In order for Level 2 analysis to yield reliable results, it is necessary to enhance the frequency resolution of the acquired data. To do so, the acquired vibration data (20,480 samples) was zero-padded to the next 2^n value, which resulted in 32,768 total data points providing a satisfactory frequency resolution that is sufficient to produce accurate results. A suitable hunting range is utilized to identify all the defect frequencies and their harmonics. Detailed information regarding this process can be found elsewhere [8]. Table 1 summarizes the results of the Level 2 analysis performed on the data acquired from the inboard smart adapter (IB-SA) accelerometer at three different operating speeds and a fully loaded railcar. Utilizing a four-second sample window, the condition monitoring algorithm is proven to accurately and reliably identify the defect type within the bearing.

Table 1. Level 2 analysis results for a 4-second sample window acquired by the IB-SA accelerometer in Experiment 202.

Applied Load [%]	Speed [km/h]/[mph]	Max/Sum [%]	Highest Magnitude
100	72/45	98	Cone
100	85/53	99	Cone
100	97/60	99	Cone

Figure 9 is a re-plot of Figure 8 with the sole difference being that the vibration signatures were generated using only one second of accelerometer data (5,120 samples). Comparing the vibration profiles of Figure 8 and Figure 9, it can be observed that the RMS values are very similar in both cases, which implies that Level 1 analysis is not compromised by using 1-second sample windows as opposed to 4-second sample windows. In both cases, the bearing is determined to be defective since the RMS values are greater than the maximum threshold.

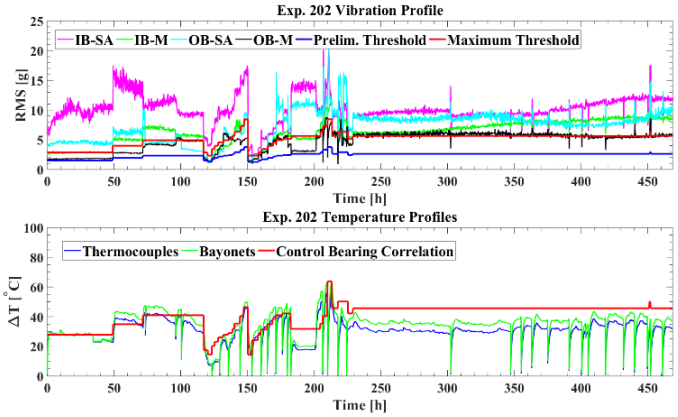

Figure 9. Vibration (1 second of data) and temperature profiles for Experiment 202.

In Level 2 analysis, it was already established that having an appropriate frequency resolution is essential to conduct an accurate and reliable analysis. In order to determine the optimal frequency resolution needed to achieve a positive identification of the defect type, the one-second accelerometer raw data (5,120 samples) was zero-padded to 2^n of 8,192, 16,384, and 32,768 data points. Table 2 summarizes the Level 2 analysis results obtained from the three different zero-padded data sets.

Table 2. Level 2 analysis results for a 1-second sample window acquired by the IB-SA accelerometer in Experiment 202.

Applied Load [%]	Speed [km/h]/[mph]	Max/Sum [%]	Highest Magnitude
Case I: 8,192 Data Points			
100	72/45	65	Cone
100	85/53	74	Cone
100	97/60	87	Cone
Case II: 16,384 Data Points			
100	72/45	65	Cone
100	85/53	95	Cone
100	97/60	86	Cone
Case III: 32,768 Data Points			
100	72/45	93	Cone
100	85/53	98	Cone
100	97/60	94	Cone

Examining Table 2, the condition monitoring algorithm was successful in correctly identifying the defect type in all three zero-padding cases. However, looking at the results more closely, it is apparent that Case II gives slightly better results than Case I, and Case III generates better results than Case II based on the percentage of maximum defect frequency magnitude over the sum of all the defect frequency magnitudes. Comparing the results of Case II and Case III, one can argue that Case II provides the best results with reasonable zero-padding which is a good balance between accuracy and efficiency. This means that the improved accuracy attained by zero-padding to 32,768 data points (Case III) does not meaningfully warrant the additional computation time associated with the larger data set. Hence, it was concluded that zero-padding the one-second sample window (5,120 samples) to 16,384 data points offers the most optimal results for Level 2 analysis in terms of accuracy and efficiency.

Experiment 221

Now that parameters have been established for analyzing the one-second sample window of accelerometer data, an experiment was carried out to assess the efficacy of the wireless onboard condition monitoring device in accurately and reliably identifying a defective bearing as well as the defect type.

In Experiment 221, a class F bearing with a cup (outer ring) spall located at the inboard raceway of the bearing was run on the single bearing test rig. Prior to testing, the cup spall size was initially 3.76 cm^2 (0.58 in^2), as pictured in Figure 10. The main objective of this experiment was to evaluate the performance of the wireless onboard condition monitoring module as compared to the wired accelerometers. The wireless module was affixed on

the outboard smart adapter (OB-SA) location, whereas, the three wired 70g accelerometers were positioned on the inboard smart adapter (IB-SA), inboard mote (IB-M), and outboard smart adapter (OB-SA) locations. This setup allowed for a direct comparison between the wireless module versus the wired accelerometer that was placed at the same location (i.e., OB-SA). Data was collected for two different speeds at two loading conditions simulating an empty and a full freight railcar.

Figure 10. Initial cup spall on the bearing inboard raceway.

Figure 11 presents the temperature and vibration signatures acquired during Experiment 221. As demonstrated earlier, the operating temperature of the bearing remained below the threshold value (red line) throughout the experiment exhibiting no abnormal operation or bearing defect. Note that the RMS values plotted in the figure were calculated from 4-second sample windows acquired by the three wired accelerometers, whereas, the RMS values for the wireless modules were calculated from 1-second sample windows. The results shown are very promising as RMS values for both wired accelerometers placed in the smart adapter (SA) locations are very comparable to the RMS values for the wireless module. Moreover, both wired and wireless devices indicate that the bearing is possibly defective (Level 1 analysis) since the RMS values are above the maximum threshold represented by the solid red line.

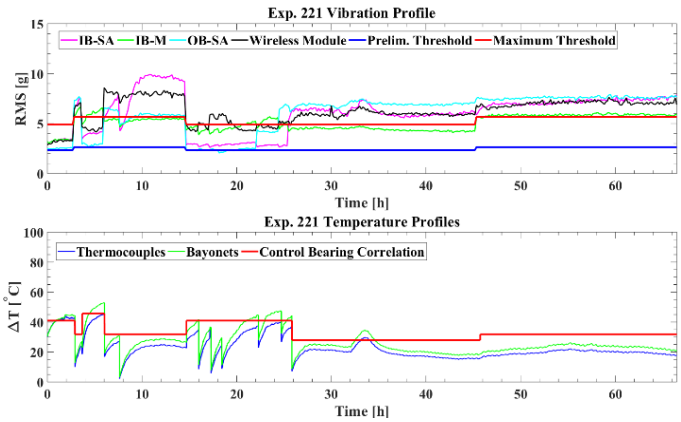

Figure 11. Vibration and temperature profiles for Experiment 221.

Table 3 and Table 4 summarize, respectively, the Level 2 analyses performed on the 4-second sample windows acquired from the three wired accelerometers and the 1-second sample windows collected by the wireless onboard module.

Table 3. Level 2 analysis of 4-second sample windows for the three wired accelerometers used in Experiment 221.

Applied Load [%]	Speed [km/h]/[mph]	Max/Sum [%]	Highest Magnitude
Outboard Smart Adapter (OB-SA)			
17	85/53	100	Cup
17	97/60	100	Cup
100	85/53	98	Cup
100	97/60	100	Cup
Inboard Smart Adapter (IB-SA)			
17	85/53	100	Cup
17	97/60	100	Cup
100	85/53	99	Cup
100	97/60	100	Cup
Inboard Mote (IB-M)			
17	85/53	100	Cup
17	97/60	100	Cup
100	85/53	96	Cup
100	97/60	100	Cup

Table 4. Level 2 analysis of 1-second sample windows for the wireless onboard module used in Experiment 221.

Applied Load [%]	Speed [km/h]/[mph]	Max/Sum [%]	Highest Magnitude
Case I: 8,192 Data Points			
17	85/53	47	Cup
17	97/60	51	Cup
100	85/53	61	Cup
100	97/60	96	Cup
Case II: 16,384 Data Points			
17	85/53	61	Cup
17	97/60	64	Cup
100	85/53	68	Cup
100	97/60	97	Cup
Case III: 32,768 Data Points			
17	85/53	75	Cup
17	97/60	77	Cup
100	85/53	69	Cup
100	97/60	96	Cup

Examining the results presented in Table 3 and Table 4, it is apparent that all four accelerometers (three wired and one wireless) have correctly identified the defect type (fourth column in each table). However, inspecting the results more closely, one can notice that the 4-second sample windows collected by the three wired accelerometers detect the defect type with more *certainty* than the 1-second sample windows acquired by the wireless onboard module based on the "Max/Sum [%]"

percentages given in third column of both tables. Nevertheless, it is rational to state that the 1-second sample windows collected by the wireless onboard module and zero-padded to 16,384 data points adequately identify the defect type albeit with less certainty than the 4-second sample windows. More importantly, it is evident that the detection certainty for the 1-second sample windows improves markedly for a full railcar at higher speeds, which are the more critical operating conditions in rail service.

CONCLUSIONS

One major drawback of the current wayside condition monitoring systems in use today is that they are reactive in nature. This means that they normally only detect defective bearings as they are nearing the end of their lifecycle. Relying solely on temperature, Hot-Box Detectors (HBDs) are not effective in identifying bearing defects at an early stage as the operating temperatures of defective bearings do not usually exhibit abnormal behavior until the defects have reached a critical size and catastrophic failure is imminent. Similarly, TADS™ are programmed to detect "growlers", which are bearings that have defects that cover 90% of the contact raceway surface area, and there are only 30 of these systems in use in North America.

To address the shortcomings of the current condition monitoring systems, the UTCRS research team has developed a vibration-based bearing condition monitoring system that can effectively assess the health of bearings and detect defects at an early stage of formation and propagation to allow for proactive maintenance to be performed. The wired version of the condition monitoring system has been validated through rigorous laboratory testing as well as a field test carried out at TTCI. Currently, the wired system utilizes four second sample windows (20,480 samples) that are zero-padded to 32,768 data points to accurately and reliably assess the bearing health and identify the type of defect (if any). The power consumption associated with the analyses will limit the battery life in the developed wireless version of the onboard condition monitoring module. Hence, this study focused on two aspects; first, it was important to investigate whether the analyses can produce accurate and reliable data utilizing only one second worth of data as opposed to four seconds, thus, reducing power consumption; and second, provide proof of concept validation for the wireless onboard module by directly comparing its performance to the wired version of the system.

The results of this study clearly demonstrate that the wireless onboard condition monitoring module that utilizes one-second sample windows can accurately assess the bearing health and identify the correct defect type, albeit with a lower certainty level than the wired system that uses four-second sample windows. Three different zero-padding cases for the Level 2 algorithm analysis were examined. Results indicate that collecting one-second of data that is zero-padded to 16,384 data points is the most efficient and effective method to assess the bearing health and identify the defect type (if any) using the wireless onboard module. However, further improvements to the condition monitoring algorithm will be sought in order to achieve better certainty in identifying the defect type at lower speeds and railcar loads.

ACKNOWLEDGMENTS

This study was made possible by funding provided by The University Transportation Center for Railway Safety (UTCRS), through a USDOT Grant No. DTRT 13-G-UTC59.

REFERENCES

[1] "Railway Bearings | Railway Bearings in India - NBC Bearings Jaipur." https://www.nbcbearings.com/railway-Products.php

[2] H. Wang, T.F. Conry, C. Cusano, 1996. "Effects of cone/axle rubbing due to roller bearing seizure on the thermomechanical behavior of a railroad Axle." *Journal of Tribology*, Vol. 118, pp. 311-319.

[3] DataTraks Secures Contract to Manage TADS for TTCI | built in Colorado. Web. https://www.builtincolorado.com/blog/datatraks-secures-contract-manage-trackside-acoustic-detection-system-tads

[4] C. Tarawneh, L. Sotelo, A. Villarreal, N. De Los Santos, R. Lechtenberg, R. Jones, 2016. "Temperature profiles of railroad tapered roller bearings with defective inner and outer rings." *Proceedings of the 2016 Joint Rail Conference*, Columbia, SC, April 12-15.

[5] N. De Los Santos, R. Jones, C. Tarawneh, A. Fuentes, and A. Villarreal, 2017. "Development of prognostic techniques for surface defect growth in railroad bearing rolling elements." *Proceedings of the 2017 ASME Joint Rail Conference*, Philadelphia, PA, April 4-7.

[6] J. Montalvo, C. Tarawneh, and A. Fuentes, 2018. "Vibration-based defect detection for freight railcar tapered-roller bearings." *Proceedings of the 2018 ASME Joint Rail Conference*, Pittsburgh, PA, April 18-20.

[7] C. Tarawneh, J. Lima, N. De Los Santos, and R. Jones, 2019. "Prognostics models for railroad tapered-roller bearings with spall defects on inner or outer rings." *Tribology Transactions*, Vol. 62, No. 5, pp. 897-906. https://doi.org/10.1080/10402004.2019.1634228

[8] J. Montalvo, 2019. "Defect detection algorithm optimization for use in freight railcar service." Master's Thesis, Mechanical Engineering Department, University of Texas Rio Grande Valley.

